Int. J. Electrochem. Sci., 16 **(2021)** Article ID: 21043, doi: 10.20964/2021.04.45

International Journal of
ELECTROCHEMICAL
SCIENCE
www.electrochemsci.org

Short Communication

Preparation of Three-dimensional Mesoporous Carbon Electrode Materials as Electrocatalysts for Hydrogen Evolution Reaction

Zhengping Zhao[1,2], Jiahao Wang[2], Xuan Yu[1], Haojie Li[1], Leiting Han[1], Zhiquan Wang[1], Dan Qiao[1], Mingqiang Zhong[2] and Xiufang Chen[3]*

[1] Zhijiang College, Zhejiang University of Technology, Hangzhou 310014, China
[2] College of Materials Science and Engineering, Zhejiang University of Technology, Hangzhou 310014, China
[3] National Engineering Lab for Textile Fiber Materials & Processing Technology, College of Materials Science and Engineering, Zhejiang Sci-Tech University, Hangzhou 310018, China
[*]E-mail: sjzhaolei@163.com

Received: 30 November 2020 / *Accepted:* 26 January 2021 / *Published:* 28 February 2021

In order to improve the electrochemical performance of hydrogen evolution electrode, this paper presents a new method of the preparation of the negative electrode materials with high activity of hydrogen evolution.8 Based on the principle of self-assembly, polyphosphazene microspheres were prepared by precipitation polymerization and carbonized in N_2 atmosphere to form blank porous carbon spheres with excellent electrical conductivity, good physical/chemical stability and outstanding absorption performance. Then NiO/Ni@C-PZS were prepared by chemical precipitation method and carbonization loading method, and labeled as sample A and sample B, respectively. It was observed that, compared with the blank carbon spheres, sample A and sample B had higher hydrogen evolution activities by electrochemical measurement. Under the same scan rate, the capacitance performance of sample A and sample B are improved significantly and have obvious redox peaks. It can be found from the LSV that the hydrogen evolution overpotential of sample A is 0.4 V (vs. RHE), and the η of sample A is basically unchanged after 100 cycles, which indicates that sample A has good cycle stability. The result that the tafel slope of sample B is only 81 $mV \cdot dec^{-1}$, far lower than the 122 $mv \cdot dec^{-1}$ of C-PZS, indicating that the existence of NiO/Ni plays an important role in hydrogen evolution activity of NiO/Ni@C-PZS electrodes and the hydrogen evolution reaction is consistent with the Volmer-Heyrovsky mechanism.

Keywords: Hydrogen evolution electrode, Porous carbon material, Electrocatalysis

1. INTRODUCTION

Petroleum, coal, natural gas and other petrochemical resources have promoted the development of human society but also brought many adverse effects such as greenhouse effect, acid rain, thus prompting people to seek clean, environmentally friendly as well as renewable energy sources.[1] Among the many alternatives to traditional energy, hydrogen energy with high efficiency, no pollution and easy storage has been regarded as the cleanest energy for a long time. [2]

After combustion, hydrogen produces only water and does not cause any pollution. The combustion calorific value of hydrogen is 1.21×105 kJ/kg that is 3 times of gasoline and 4 times of standard coal. About 70% of the earth's surface is covered with water, so hydrogen is abundant.

Electrolytic water reaction is a rather practical way of producing hydrogen. Electrolysis reaction seems easy but there are many steps which lead to the accumulation of energy barrier and slow down the reaction rate. It is the reason that the theoretical decomposition voltage of electrolytic water only needs 1.23 V, the actual decomposition voltage needs 2-3 V. [3]

The specific mechanism of hydrogen evolution reaction (HER) includes the following three elementary reactions. [4-5]

Electron transfer (Volmer reaction)

$M+H_3O+e^- \longrightarrow MHads+H_2O$ (Acid electrolyte) （1-1）

$H_2O+e^-+M \longrightarrow MHads+OH^-$(Neutral or alkaline electrolyte) （1-2）

Electrochemical desorption (Heyrovsky reaction)

$H_3O+e^-+MHads \longrightarrow H_2\uparrow+H_2O$(Acid electrolyte) （1-3）

$MHads+e^-+H_2O \longrightarrow M+ H_2\uparrow+OH^-$(Neutral or alkaline electrolyte)（1-4）

Complex desorption (Tafel reaction)

$2MHads \longrightarrow 2M+H_2\uparrow$(Acid Neutral or alkaline electrolyte) （1-5）

M as a metal active point.

The hydrogen evolution reaction begins from Volmer adsorption firstly. One hydrogen proton obtains an electron and combines with the active site on the electrode surface to form MHads. MHads can carry out either Heyrovsky reaction or Tafel reaction. [6] In the process of desorption, the rate of hydrogen evolution of the Tafel reaction is much higher than Heyrovsky reaction. Namely for improvement of the catalytic activity wholly, it is necessary to increase the number of metal active sites as much as possible.

The cathodic electrode materials should have excellent electrocatalytic activity for the HER. Noble metal Pt is the most active materials. But for industrial applications, Pt is too expensive. Among studied transition metals like Fe, Co and Ni. Ni has good hydrogen evolution performance because of its individual electronic structure. Its unpaired d orbital electrons can be paired with hydrogen 1s orbital electron to form moderate M-H bond. [7-8] However, pure nickel is not suitable being used as hydrogen evolution electrode for its poor conductivity and small specific surface area that exposed active sites. [9] Therefore, many scholars focus on changing the structure of Ni-based alloys designing highly electrocatalytic materials by nano-modification and composite of porous materials.

Hou prepared Ni0.05 -MoS2/G by one-step hydrothermal method. [8] The results show that the Tafel slope of the prepared $Ni_{0.05}$-MoS_2/G is 50.8 $mV \cdot dec^{-1}$. Wang deposited GO and Ni nanoparticles

on Ni foam by high-gravity electrodeposition. The η of composite electrode prepared is 184mV and The Tafel slope is 77 $mV \cdot dec^{-1}$ at 100 $mA \cdot cm^{-2}$. [11] Graphene supplies excellent conductivity and avoids the agglomeration of Ni nanoparticles, greatly enhancing the number of metal active centers.

Polyphosphazenes (PZS) is a kind of high molecular polymer with alternate P and N as the main chain and two organic side groups connected to P [12]. Zhu synthesized polyphosphazene nanotubes with12~20nm inner diameter and 1~2μm uniform length by ultrasonic reaction using HCCP and BPS as comonomers, THF as solvent and TEA as catalyst. Zhu found that on the basis of the original method, polyphosphazene nanospheres with uniform particle size was successfully prepared by using acetonitrile as solvent. On the basis of Zhu's research. Fu further proposed the principle of in situ template induced self-assembly. The polycondensation reaction of HCCP and BPS generates HCl, which is adsorbed by TEA and becomes TEACL, which is used as template to induce polyphosphazenes to self-assemble. [13]

Without activator, Polyphosphazene can spontaneously form multi-stage porous carbon structure by carbonization. Porous carbon structure can improve the permeability of electrolyte and has the characteristics of good conductivity, high ion mobility and large specific surface area. In addition, A small number of heteroatoms such as N, P, S were in-situ doped into the carbon skeleton network after carbonization, which changed the local charge density of the materials thus generating more active sites, further improving the catalytic activity of the materials. [14-15]

Ni-based alloys have represented high catalytic activity in HER and exhibited better catalytic capability than single Ni catalyst for synergistic electronic effect among alloys. Then multicomponent Ni-based alloy materials including a nonmetallic element are the subjects of this paper. The role of NiO/Ni on the electrodes and the preparation method of composite electrode material ware studied systematically. Firstly, polyphosphazene microspheres were prepared by precipitation polymerization and carbonized in N_2 atmosphere to form blank porous carbon spheres. Then NiO/Ni@C-PZS were prepared by chemical precipitation method and carbonization loading method, labeled as sample A and sample B, respectively. Finally, through electrochemical tests including CV and LSV, the gained substances were tested to analyze electrochemical properties including the hydrogen evolution overpotential, cyclic stability as well as reaction mechanism.

2. EXPERIMENTAL SECTION

2.1 Preparation of C-PZS

Add 0.345g HCCP and 0.595g BPS to 500ml acetonitrile, then put the mixed solution in a high-power sonicator with 300W power for one hour before adding 15ml of triethylamine and continue sonication for 3 hours. The solution after sonication was centrifuged at 3000 rpm to obtain PZS microspheres. The microspheres were dried in a vacuum drying oven at 70°C for 24 hours after washed with deionized water as well as ethanol for 3 times. Blank C-PZS was obtained by carbonizing PZS microspheres in tube furnace under N_2 atmosphere and grounding into powder agate mortar.

2.2 NiO/Ni@C-PZS Preparation

0.3g blank C-PZS was magnetically stirred in 1M sodium hydroxide solution for 15mins to obtain carbon spheres adsorbing OH^-. Then the carbon spheres were ultrasonic treated with 300 W power for 20 minutes in the solution blending of 0.24g $Ni(NO3)_2 \cdot 6H_2O$ and 100ml water.

According to chemical precipitation way, Ni^{2+} could be well adsorbed on the carbon spheres through the interaction of ionic bonds **Error! Reference source not found.**. The carbon spheres were dried in vacuum drying oven at 70°C for 24 hours after washed with deionized water for 3 times. After drying, carbonize the carbon spheres in tube furnace under N_2 atmosphere and ground into powder in agate mortar to obtain NiO/Ni@C-PZS (Sample A).

According to carbonization loading method, add 0.3g blank C-PZS and 3.63g $Ni(NO3)_2 \cdot 6H_2O$ to 1M NaOH to obtain composite of C-PZS and $Ni(OH)_2$. Graphitize composite to obtain NiO/Ni@C-PZS (Sample B).

2.3 Characterization and testing

Working electrode preparation: add 1mg sample to 0.9mL ethanol and 0.1ml Nafion solution. Evenly dropped the slurry on the carbon paper ($1\times1cm^2$) with a pipette after stirring for one hour. The infrared lamp is used to speed up the drying of carbon paper. Working electrode was prepared by repeating above process until the carbon paper completely absorbed 1ml solution.

The electrochemical workstation used is RST5202F electrochemical workstation produced by Zhengzhou Shiruisi Instrument Technology Co., Ltd. The test system used was a three-electrode system, with pair electrode of graphite electrode, reference electrode of extremely saturated silver chloride (Ag/AgCl) electrode and working electrode of material above prepared. The test environment was 1M KOH alkaline electrolyte at room temperature. [16]

Cyclic Voltammetry (CV) is a commonly used electrochemical method. It controls the variation of scanning voltage and records the potential current curve by triangle waveform scanning. The scanning rates of the test were 0.01V/s, 0.02V/s, 0.05V/s, 0.1V/s and 0.5V/s, respectively. The scanning voltage range was -0.2-0.6V and the number of cycles was 10.

Linear Sweep Curve (LSV) is a curve that value of the current varies with the linear voltage at a linear voltage. The scanning voltage range is -0.6-0.1V and the scanning rate is 0.002V/s.

When Ag/AgCl electrode is used as the reference electrode and the filling solution is saturated KCl, the Nernst equation can be transformed into:

$$E(RHE)=E(Ag/AgCl)+0.0592pH+0.197 \quad (2\text{-}1)$$

All the potentials are relative to the reversible hydrogen electrode (RHE), that is, 0.197 V should be added to E(Ag/AgCl). The obtained electrode potential is exactly hydrogen evolution overpotential.

According to the measured LSV curve, draw the Tafel curve and calculate the Tafel slope. [17]

Tafel formula is as follows,

$$\eta=A+B\log|j| \quad (2\text{-}2)$$

This formula is only applicable to the case of higher j and describes the relationship between η and j. The Tafel slope B in the formula is an important parameter to judge kinetics of electrode process. If the Tafel slope is about 120 $mV \cdot dec^{-1}$, the Volmer adsorption is a rate control step. If the Tafel slope is about 40 $mV \cdot dec^{-1}$, the Heyrovsky reaction is a rate control step. If the Tafel slope is about 30 $mV \cdot dec^{-1}$, the Tafel reaction is a rate control step. Generally, the lower the Tafel slope is, the better the performance of hydrogen evolution of catalyst. [18]

3. RESULTS AND DISCUSSION

Figure 1 show the.CV curves of blank C-PZS、NiO/Ni@C-PZS (Sample A) and NiO/Ni@C-PZS (Sample B) at a scanning rate of 0.1V/s. It can be seen from Figure 1 that sample A and blank C-PZS are symmetrical. At the same potential, the j of sample A is slightly increased compared with blank C-PZS, which indicates the capacitance is obviously improved. [19]

It is obvious that the cyclic voltammetry curve of sample B shows a symmetrical redox peak due to the addition of NiO. These two peaks indicate that the electron transfer is reversible. The appearance of anode peak is due to the oxidation reaction. NiO and OH^- combine and lose electrons, becoming NiOOH. The appearance of cathode peak is just the opposite. NiOOH gets electrons and generates NiO and OH^-. The specific redox reaction is shown in the following formula:

$$NiO+OH^- \leftrightarrow NiOOH+e^- \quad (3\text{-}1)$$

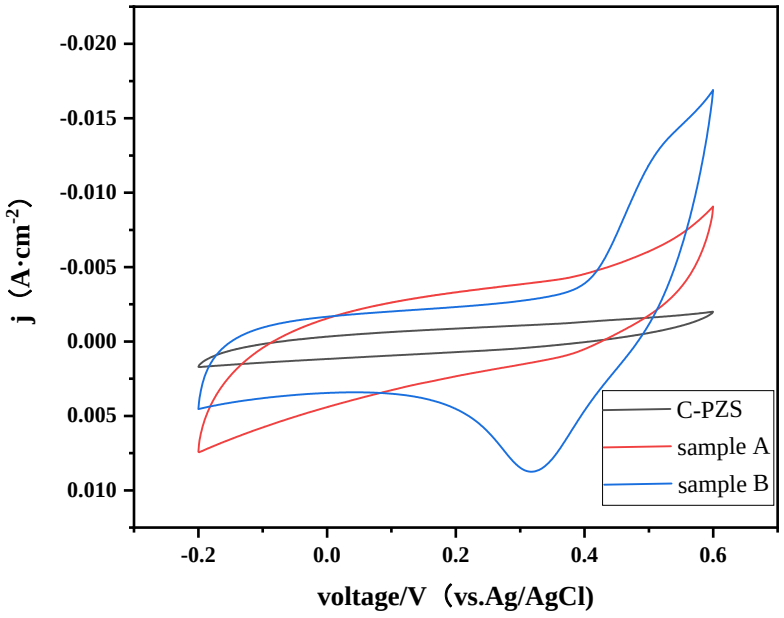

Figure 1. Cyclic voltammetry curves of blank C-PZS、Sample A and Sample B at a scanning rate of 0.1V/s with electrolyte of 1M KOH at room temperature.

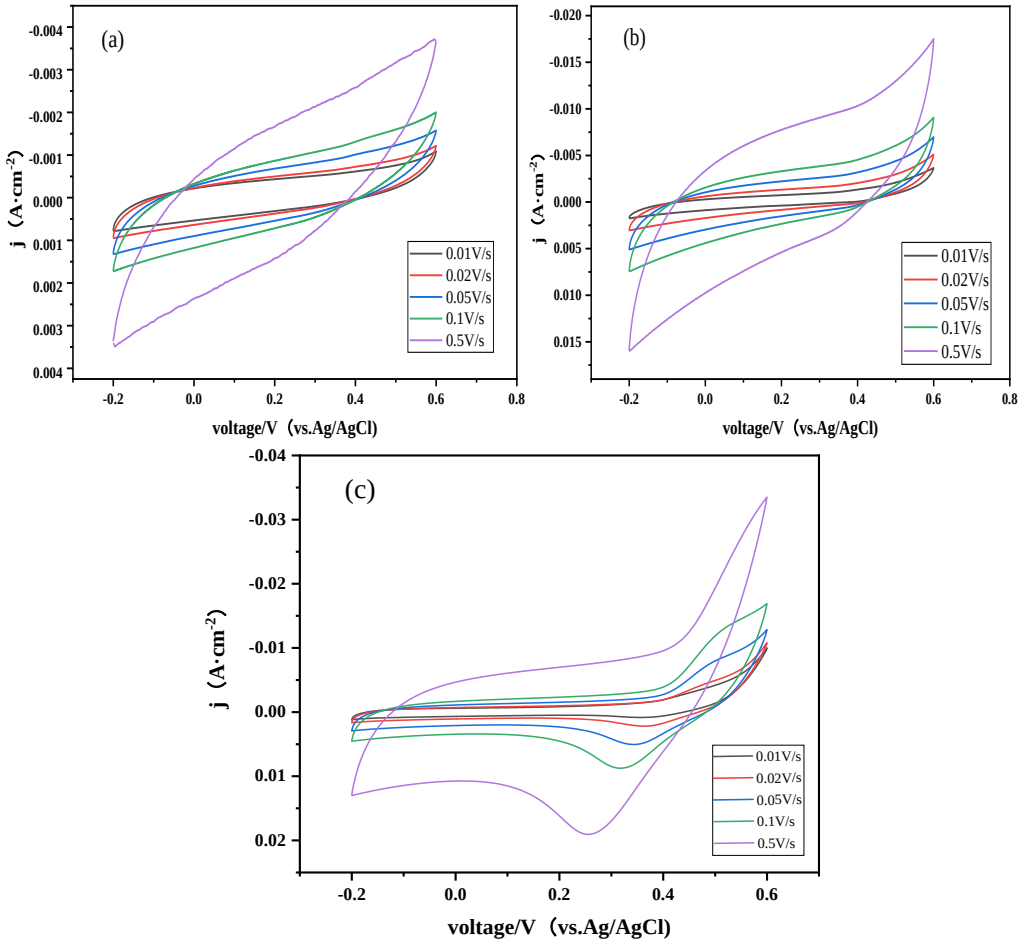

Figure 2. Cyclic voltammetry curves of (a)blank C-PZS, (b) SampleA and (c) Sample B at 0.01V/s, 0.02V/s, 0.05V/s, 0.1V/s and 0.5V/s test rates with electrolyte of 1M KOH at room temperature.

As shown in Figure 2 (a) and (b), the good symmetry of CV graphs (a) and (b) indicates the high invertibility of both the blank C-PZS and NiO/Ni@C-PZS (Sample A). It can be seen that the shape of cyclic voltammetry curve of blank C-PZS and sample A do not change with the change of scanning rate at different scanning rates, but the corresponding value of the curve changes, which indicates that blank C-PZS and sample A have the characteristics of Faraday pseudo capacitance. With the decrease of scanning rate, the redox peak of the sample becomes more and more obvious, which is due to the fact that NiO/Ni has enough time to gain and lose electrons and more NiO/Ni takes part in the redox reaction at a lower scanning rate.

In the cathode scanning area of graph (c), with the increase of scanning rate, the oxidation peak of the sample becomes more and more obvious, but when the scanning rate reaches 0.5V/s, the oxidation peak is masked, which is due to the fact that nickel oxide has enough time to gain and lose electrons and more NiO/Ni take part in the redox reaction at an appropriate scanning rate. [20] The j of sample B is much higher than that of sample A because of the high content of nickel.

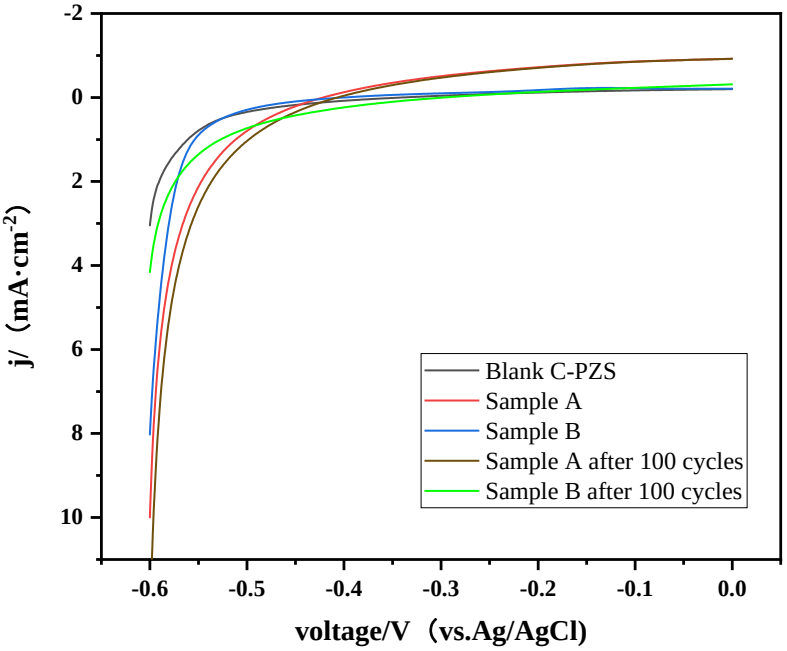

Figure 3. Cathodic polarization curves of blank C-PZS, Sample A and Sample B with electrolyte of 1M KOH at room temperature.

Fig. 3 depicts the polarization curves of blank C-PZS, Sample A and Sample B. As shown in Figure 3, The LSV curve of each sample underwent electrochemical reaction at the overpotential of about 0.4V, which was consistent with the CV.

The j of sample A is10 $mA \cdot cm^{-2}$ when η is 0.4 V, but with the increasing of the η, the j of blank C-PZS is always less than 10 $mA \cdot cm^{-2}$, far lower than sample A. Although the j of sample B increased, after 100 cycles, the j was reduced by 48%. However, under the same condition, the j of sample A increased instead, which may is attributed to the participation of NiO/Ni that have not taken part in the reaction, indicating that the cyclic stability of sample A is better than that of sample B.

Table 1. Collected HER Catalysis Data

catalyst	loading ($mg \cdot cm^{-2}$)	electrolyte	η/mV (vs.RHE)	J / $mA \cdot cm^{-2}$
NiO/Ni@C-PZS	1.0	1 M KOH	400	10
NiO/HMPC[3]	4.0	1 M KOH	190	10
Ni−Mo nitride nanosheets[22]	0.25	0.1 M $HClO_4$	200	3.5
Ni0.05 -MoS2/G[8]	4.0	0.5 M H_2SO_4	300	130
amorphous MoSx[23]	/	0.5 M H_2SO_4	200	10
Ni−Mo nanopowder[24]	1.0	2 M KOH	70	20

The hydrogen evolution activity data for NiO/Ni@C-PZS and several reported catalyst systems are compared in Table 1. The reason that the η of NiO/Ni@C-PZS is slightly higher than other reported

electrocatalysts is sample A and sample B are not the optimal formula, By adjusting the formula and further experimenting, it is promising to prepare NiO/Ni@C-PZS with high efficiency.

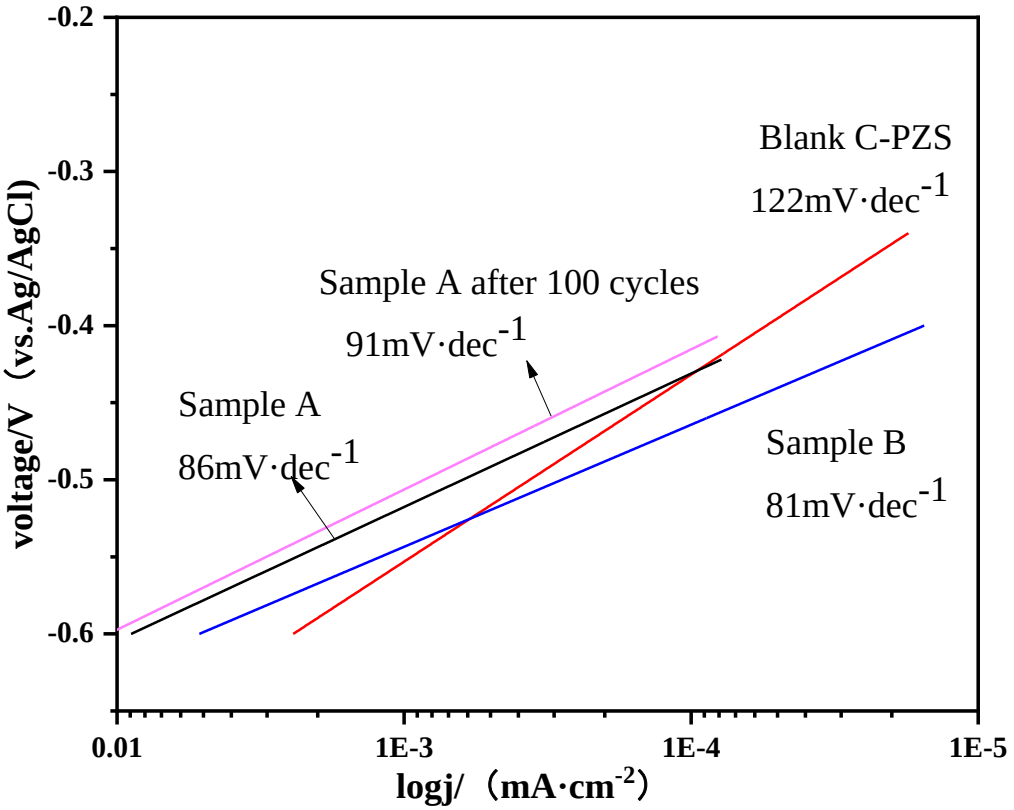

Figure 4. The Tafel curves of Blank C-PZS, Sample A, Sample B and Sample A after 100 cycles with electrolyte of 1M KOH at room temperature.

It can be seen from the Fig. 4 that the Tafel slopes of all samples are between 81-122 mV·dec^{-1}, which indicates that Heyrovsky reaction became the speed limiting step, so the number of active sites of the catalyst became the key to determine the activity of the catalyst. [20-21]. Compared with C-PZS, the Tafel slope of samples A and sample B is only 86 and 81 mV·dec^{-1}, indicating that the combination of carbon nanofibers and nickel oxide can effectively increase the catalytic performance of the sample. After 100 cycles, the tafel slope of sample A only increases to 91, indicating that sample A has excellent electrochemical stability.

4. CONCLUSIONS

NiO/Ni@C-PZS were prepared by chemical precipitation method and carbonization loading method. 2Under the same scan rate, compared with the blank C-PZS, NiO/Ni@C-PZS have improved capacitance performance and obvious redox peak. After 100 cycles, the η of sample B decreases by 48%,

while sample A remains basically unchanged, which indicates that the cyclic stability of sample A is better than sample B. The η of sample A is 0.4V, which is lower than sample B. This may be due to the fact that the NiO/Ni loaded on the chemical precipitation is evenly distributed on the carbon sphere. The result that the tafel slope of sample B is only 81 $mV \cdot dec^{-1}$, far lower than the 122 $mv \cdot dec^{-1}$ of C-PZS, indicating that the existence of NiO/Ni play an important role in hydrogen evolution activity of NiO/Ni@C-PZS electrodes and the hydrogen evolution reaction is consistent with the Volmer-Heyrovsky mechanism.

ACKNOWLEDGEMENTS
We are thankful for the Project Supported by 13th Five-Year the National key R&D projects (2017YFD0600805), Zhejiang Provincial Natural Science Foundation of China (LY21C160007) and National Natural Science Foundation of China (21504079) for the support to this research.

References

1. T. Li, G. Luo and K. Liu, *Adv. Funct. Mater.*, 51 (2018) 1805828.
2. N. T. Suen, S. F. Hung and Q. Quan, *Chem. Soc. Rev.*, 46 (2017) 337.
3. Z. P. Zhao, Z. P. Zhou and M. Q. Zhong, *Int. J. Electrochem. Sci.*, 13 (2018) 3621.
4. M. Gong, D. Y. Wang and C. C. Chen, *Nano Res.*, 9 (2016) 28.
5. A. B. Laursen, S. Kegnaes and I. Chorkendorff, *Energy Environ. Sci.*, 5 (2012) 5577.
6. M. H. Miles, G. Kissel, *J. Electrochem. Soc.*, 123 (1976) 332.
7. N. Krstaji, M. Popovi and B. Group, *J. Electroanal. Chem.*, 1 (2001) 27.
8. F. Chen, L. Wu, Z. P. Zhao, *Chinese Chem. Lett.*, 1 (2019) 197.
9. Z. P. Zhao, S. T. Shen, F. Chen. Z. P. Zhou and M. Q. Zhong, *Int. J. Electrochem. Sci.*, 14 (2019) 10058.
10. Z. P. Zhao, S. T. Shen and M. Q. Zhong, *Int. J. Electrochem. Sci.*, 15 (2020) 2739.
11. Y. Zhu, X. B. Huang and W. Z. Li, *Mater. Lett.*, 62 (2008) 1389.
12. L. X. Wang, Y. Li, M. Xia and Q. Li, *J. Power Sources*, 347 (2017) 220.
13. H. J. Qiu, Y. Ito and W. Cong, *Angew. Chem.*, 127 (2016) 14237.
14. J. R. Mckone, B. F. Sadtler, C. A. Werlang, *ACS Catal.*, 3 (2013) 166.
15. Y. Zhu, X. B. Huang and J. W. Fu, *Mater. Sci. Eng., C*, 153 (2008) 62.
16. J. Y. Ye, Li Z., Z. Dai and B. Gu, *J. Electr. Mat.*, 45 (2016) 4237.
17. L. J. Song, H. M. Meng, *Int. J. Hydrogen Energy*, 35 (2010) 10060.
18. W. Wen, J. Wu, *ACS Appl. Mater. Interfaces*, 3 (2011) 4112.
19. J. Liang, H. Hu, H. Park, *Energy Environ. Sci.*, 8 (2015) 1707.
20. F. Chen, W. Zhou, H. Yao, *Green Chem.*, 15 (2013) 3057.
21. Z. P. Zhao, Z. P. Zhou and M. Q. Zhong, *Int. J. Electrochem. Sci.*, 9 (2014) 8120.
22. W. F. Chen, K. Sasaki, C. Ma, A. I. Frenkel, *Angew. Chem., Int. Ed.*, 51(2012) 6131.
23. J. D. Benck, Z. Chen, L. Y. Kuritzky, A. J. Forman, *ACS Catal.,* 2(2012) 1916.
24. J. R. McKone, B. F. Sadtler, C. A. Werlang, *ACS Catal*., 3(2013) 166.